Journal of Biomedical Optics

BiomedicalOptics.SPIEDigitalLibrary.org

Mueller-matrix of laser-induced autofluorescence of polycrystalline films of dried peritoneal fluid in diagnostics of endometriosis

Yuriy A. Ushenko
Galina D. Koval
Alexander G. Ushenko
Olexander V. Dubolazov
Vladimir A. Ushenko
Olga Yu. Novakovskaia

SPIE.

Yuriy A. Ushenko, Galina D. Koval, Alexander G. Ushenko, Olexander V. Dubolazov, Vladimir A. Ushenko, Olga Yu. Novakovskaia, "Mueller-matrix of laser-induced autofluorescence of polycrystalline films of dried peritoneal fluid in diagnostics of endometriosis," *J. Biomed. Opt.* **21**(7), 071116 (2016), doi: 10.1117/1.JBO.21.7.071116.

Mueller-matrix of laser-induced autofluorescence of polycrystalline films of dried peritoneal fluid in diagnostics of endometriosis

Yuriy A. Ushenko,[a,*] Galina D. Koval,[b] Alexander G. Ushenko,[c,*] Olexander V. Dubolazov,[c] Vladimir A. Ushenko,[a] and Olga Yu. Novakovskaia[d]
[a]Chernivtsi National University, Department of Correlation Optics, 2 Kotsiubynskyi Street, 2 Theatre Square, Chernivtsi 58000, Ukraine
[b]Bukovynian State Medical University, Department of Forensic Medicine and Medical Jurisprudence, 2 Theatre Square, Chernivtsi 58000, Ukraine
[c]Chernivtsi National University, Department of Optics and Publishing, 2 Kotsiubynskyi Street, 2 Theatre Square, Chernivtsi 58000, Ukraine
[d]Bukovynian State Medical University, Department of Medical Physics and Biological Informatics, 2 Theatre Square, Chernivtsi 58000, Ukraine

Abstract. This research presents investigation results of the diagnostic efficiency of an azimuthally stable Mueller-matrix method of analysis of laser autofluorescence of polycrystalline films of dried uterine cavity peritoneal fluid. A model of the generalized optical anisotropy of films of dried peritoneal fluid is proposed in order to define the processes of laser autofluorescence. The influence of complex mechanisms of both phase (linear and circular birefringence) and amplitude (linear and circular dichroism) anisotropies is taken into consideration. The interconnections between the azimuthally stable Mueller-matrix elements characterizing laser autofluorescence and different mechanisms of optical anisotropy are determined. The statistical analysis of coordinate distributions of such Mueller-matrix rotation invariants is proposed. Thereupon the quantitative criteria (statistic moments of the first to the fourth order) of differentiation of polycrystalline films of dried peritoneal fluid, group 1 (healthy donors) and group 2 (uterus endometriosis patients), are determined. [DOI: 10.1117/1.JBO.21.7.071116]

Keywords: Mueller-matrix; polarization; autofluorescense; biological fluids; birefringence; statistics.

Paper 150650SSRR received Oct. 2, 2015; accepted for publication Apr. 18, 2016; published online May 18, 2016.

1 Introduction

Biological layers (tissues) including dried films (smears) of human biological fluids represent optical anisotropic media with absorption. To describe interactions of polarized light with such complex systems, more generalized approximations are required based on Mueller-matrix formalism. Nowadays many practical techniques based on the measurement and analysis of Mueller matrices of the investigated samples are applied in biological and medical research.[1–10] Laser polarimetry was formed as a separate direction of matrix optics over 10 to 15 years.[11–20] On its base, the interconnections between the set of statistical moments of the first to fourth orders, correlation, fractal, and singular parameters were determined, which characterize the distributions of Mueller-matrix elements and the parameters of linear birefringence of fibrillar protein networks of human biological tissues.[11,12] On this basis, the diagnostics of pathological changes of skin derma, epithelial, and connective tissues of women's reproductive sphere organs have been realized.[14–20]

The optical techniques of investigation of biological tissues are widespread in modern medical diagnostics. The analysis of luminescence of such objects has a special place among the optical biopsy techniques. One of the most attractive directions is the intrinsic fluorescence or autofluorescence. The applied-physics fundamentals of laser radiation usage in the tasks of diagnostics of typical pathological processes by laser-induced fluorescence spectroscopy were elaborated.[21,22]

Another important direction in the field of fluorescence diagnostics is the investigation of biological fluids of human organs such as whole blood, including serum and plasma, urine, bile, saliva, and others.[23–25] An important role here is dedicated to the analysis of induced radiation of various endogenous fluorophores. One of the most promising is the porphyrin emission analysis. Porphyrin molecules are microcycles of four pyrrole rings. The most common endogenous fluorophores of this type are protoporphyrin, coproporphyrin, and uroporphyrin, which accumulate in the red blood cells, serum, and other biological fluids.[26] Most diagnostic methods using porphyrin fluorescence are based on the fact that the amount of porphyrin IX in erythrocytes in pathological conditions of human bodies increases by 10 to 15 times. The diagnostic application of the method of spectral fluorometry of whole blood, including serum and plasma, in oncology and other areas of medicine is based on the effect of increasing fluorescence intensity of the porphyrins in the "red" range of the spectrum.[27,28]

However, in the modern literature there are a comparatively small number of publications[20,29–31] on polarization manifestations of fluorescence effects in biological tissues and fluids. Thus, the topical task of complex unification of diagnostic potentiality of both the techniques of laser polarimetry and laser autofluorescence proves to be important.

*Address all correspondence to: Yuriy A. Ushenko, E-mail: yuriyu@gmail.com

1083-3668/2016/$25.00 © 2016 SPIE

Our research is aimed at studying the efficiency of polarization-fluorescence diagnostics of uterus endometriosis without using conventional biopsy. A biopsy of the uterus wall by laparoscopy is the gold standard for the differential diagnosis of endometriosis. However, this method has a number of limitations and drawbacks, such as diagnostic errors during sampling and subjective perception of histological changes. In addition, the traditional method of biopsy is painful (traumatic) for the patient and exposes the risk of complication. For noninvasive diagnostics of endometriosis methods of radiography, ultrasonic scanning, hysteroscopy, and exogenous and endogenous fluorescent diagnostics of cells and tissues of the uterus were developed. These methods allow detection of endometriosis at late (nodular) stages.[32–35] Therefore, elaboration of an objective, low-cost, and express screening method of diagnostics of endometriosis at early stages (before nodular stage) of pathology of the female reproductive system with accuracy close to the gold standard has become a topical task.

As a specific direction insufficiently studied in the modern literature, we will consider the possibilities of polarization analysis of fluorescence of intraperitoneal fluid smears. The main focus of this article is on the possibility of the endometriosis diagnostics by the use of polarization analysis of porphyrins fluorescence of polycrystalline films of dried peritoneal fluid (fluorescence analysis of other endogenous fluorophores is not the subject of this paper).

2 Theoretical Background

From the optical point of view, the porphyrin IX has the following spectral maxima of absorption: $\lambda_{\text{abs}}^{(1)} = 0.405\ \mu$m, $\lambda_{\text{abs}}^{(2)} = 0.671\ \mu$m, and of fluorescence: $\lambda_{\text{fluor}}^{(1)} = 0.623\ \mu$m, $\lambda_{\text{fluor}}^{(2)} = 0.675\ \mu$m, $\lambda_{\text{fluor}}^{(3)} = 0.705\ \mu$m.[26] The most intense is the maximum of $\lambda_{\text{fluor}}^{(1)} = 0.623\ \mu$m. In this research, we shall confine ourselves to consideration of the spectral region $\lambda_f = 0.63$ to $0.65\ \mu$m. Excitation of autofluorescence was performed using a blue laser with $\lambda = 0.405\ \mu$m, coinciding with the maximum of porphyrin absorption.

The formation of laser polarization fluorescence of the polycrystalline film is based on:

- the mechanisms of optically anisotropic absorption (linear and circular dichroism);[36]
- the fluorescence of porphyrin molecules ("linear" oscillators) and polycrystalline networks ("elliptical" oscillators) formed by them;[37,38]
- the mechanisms of phase anisotropy (linear and circular birefringence of polycrystalline networks) that modulate fluorescent radiation.[38]

The above-mentioned scenario can be described using Mueller-matrix formalism.

1. Anisotropic absorption: Polycrystalline networks of film of dried peritoneal fluid formed by spatially oriented molecules are characterized by linear dichroism. Optical manifestations of this mechanism are characterized by the following Mueller matrix:[11,36]

$$\{\Psi\} = \begin{Vmatrix} 1 & \psi_{12} & \psi_{13} & 0 \\ \psi_{21} & \psi_{22} & \psi_{23} & 0 \\ \psi_{31} & \psi_{32} & \psi_{33} & 0 \\ 0 & 0 & 0 & \psi_{44} \end{Vmatrix},$$

$$\text{where } \psi_{ik} = \frac{1}{1+\Delta\tau} \times \begin{cases} \psi_{12} = \psi_{21} = (1-\Delta\tau)\cos 2\gamma; \\ \psi_{13} = \psi_{31} = (1-\Delta\tau)\sin 2\gamma; \\ \psi_{22} = (1+\Delta\tau)\cos^2 2\gamma + 2\sqrt{\Delta\tau}\sin^2 2\gamma; \\ \psi_{23} = \psi_{32} = (1-\sqrt{\Delta\tau})^2 \cos 2\gamma \sin 2\gamma; \\ \psi_{33} = (1+\Delta\tau)\sin^2 2\gamma + 2\sqrt{\Delta\tau}\cos^2 2\gamma; \\ \psi_{44} = 2\sqrt{\Delta\tau}. \end{cases} \quad (1)$$

Here $\Delta\tau = (\tau_x/\tau_y)$, $\begin{cases} \tau_x = \tau\cos\rho; \\ \tau_y = \tau\sin\rho \end{cases}$, τ_x, τ_y are absorption coefficients of linearly polarized orthogonal components of the amplitude of laser radiation, and γ is the orientation of the optical axis of biological crystals in the plane of polycrystalline film. In the presence of a spiral-like structure of molecules (protein primary structures, such as alpha helixes of albumin, globulin, fibrin, and porphyrin macrocycles), circular dichroism is formed. Optical manifestations of this mechanism are described by the following matrix operator:

$$\{\Phi\} = \begin{Vmatrix} 1 & 0 & 0 & \varphi_{14} \\ 0 & \varphi_{22} & 0 & 0 \\ 0 & 0 & \varphi_{33} & 0 \\ \varphi_{41} & 0 & 0 & 1 \end{Vmatrix},$$

$$\text{where } \varphi_{ik} = \begin{cases} \varphi_{22} = \varphi_{33} = \frac{1-\Delta g^2}{1+\Delta g^2}; \\ \varphi_{14} = \varphi_{41} = \pm\frac{2\Delta g}{1+\Delta g^2}. \end{cases} \quad (2)$$

Here $\Delta g = [(g_{\otimes} - g_{\oplus})/(g_{\otimes} + g_{\oplus})]$, $g_{\otimes}$, $g_{\oplus}$ are absorption coefficients of left- ($\otimes$) and right- ($\oplus$) circularly polarized components of the amplitude of laser radiation.

2. (Auto)fluorescence: Polarization manifestations of porphyrin fluorescence are characterized by the Mueller matrix presented in Refs. 37 and 38 for the ensembles of such molecules:

$$\{F\} = \begin{Vmatrix} 1 & f_{12} & 0 & 0 \\ f_{21} & f_{22} & 0 & 0 \\ 0 & 0 & f_{33} & 0 \\ 0 & 0 & 0 & f_{44} \end{Vmatrix},$$

$$\text{where } f_{ik} = f_{11}^{-1} \begin{cases} f_{11} = a - b\sin^2\vartheta; \\ f_{12} = F_{21} = -b\sin^2\vartheta; \\ f_{22} = b(1+\cos^2\vartheta); \\ f_{33} = 2b\cos\vartheta; \\ f_{44} = 2c\cos\vartheta. \end{cases} \quad . \quad (3)$$

Here ϑ is the angle of scattering; a and b are the interrelated constants determined by the following relations for the system of linear oscillators in an isotropic medium:

$$a = 0.5(1 + \langle \cos^2 \varepsilon \rangle), \tag{4}$$

$$b = 0.25(3\langle \cos^2 \varepsilon \rangle - 1), \tag{5}$$

where ε is the angle between the radiation of dipole and polarization azimuth of illuminating beam. In Ref. 38 two boundary values of $\langle \cos^2 \varepsilon \rangle$ are determined:

- system of collinear dipoles: $\langle \cos^2 \varepsilon \rangle = 3/5$;
- system of randomly oriented dipoles: $\langle \cos^2 \varepsilon \rangle = 1/3$.

Parameter c is related to the optical activity of molecules. Here the radiation of the ensembles of optically active molecules as an ensemble of elliptical oscillators is considered. In the limiting case the value of the mentioned parameter reaches $c = 5/16$.

3. Phase modulation of porphyrin fluorescence: Fluorescent radiation of linear and elliptical oscillators [Eqs. (3)–(5)] formed as a result of absorption mechanisms [relations (1) and (2)] is distributed in the volume of the optically anisotropic polycrystalline film. As a result a phase modulation of such a radiation occurs. Optical activity $\{\Omega\}$ of amino acids and polypeptide chains formed by them, as well as birefringence $\{D\}$ of polycrystalline networks, are the main mechanisms of such a modulation:[11,36]

$$\{\Omega\} = \begin{Vmatrix} 1 & 0 & 0 & 0 \\ 0 & \omega_{22} & \omega_{23} & 0 \\ 0 & \omega_{32} & \omega_{33} & 0 \\ 0 & 0 & 0 & 1 \end{Vmatrix},$$

$$\text{where } \omega_{ik} = \begin{cases} \omega_{22} = \omega_{33} = \cos 2\theta; \\ \omega_{23} = -\omega_{32} = \sin 2\theta. \end{cases} \tag{6}$$

Here θ is the rotation angle of the polarization plane of fluorescent radiation:

$$\{D\} = \begin{Vmatrix} 1 & 0 & 0 & 0 \\ 0 & d_{22} & d_{23} & d_{24} \\ 0 & d_{32} & d_{33} & d_{34} \\ 0 & d_{42} & d_{43} & d_{44} \end{Vmatrix},$$

$$\text{where } d_{ik} = \begin{cases} d_{22} = \cos^2 2\gamma + \sin^2 2\gamma \cos \delta; \\ d_{23} = d_{32} = \cos 2\gamma \sin 2\gamma (1 - \cos \delta); \\ d_{33} = \sin^2 2\gamma + \cos^2 2\gamma \cos \delta; \\ d_{24} = -d_{42} = \sin 2\gamma \sin \delta; \\ d_{34} = -d_{43} = \cos 2\gamma \sin \delta; \\ d_{44} = \cos \delta. \end{cases} \tag{7}$$

Here δ is the phase shift between linearly polarized orthogonal components of the fluorescent radiation amplitude.

Taking into account all mechanisms of optically anisotropic absorption of laser radiation and phase modulation of porphyrin fluorescent radiation considered above, the resulting matrix of a polycrystalline film can be written as follows:

$$\{R\} = \{D\}\{\Omega\}\{F\}\{\Psi\}\{\Phi\} = \begin{Vmatrix} 1 & r_{12} & r_{13} & r_{14} \\ r_{21} & r_{22} & r_{23} & r_{24} \\ r_{31} & r_{32} & r_{33} & r_{34} \\ r_{41} & r_{42} & r_{43} & r_{44} \end{Vmatrix}. \tag{8}$$

The analysis of matrix Eq. (8) shows that elements r_{ik} characterize superposition of the mechanisms of linear ($\Delta\tau$, γ) and circular (Δg) dichroism; fluorescence of linear ($f_{12;21;22;33}$) and elliptical (f_{44}) oscillators following the phase modulation of such oscillation by optically active molecules (θ) and birefringent (γ, δ) networks of such molecules. At that point the informational content of matrix elements is different. The ensemble of elements $r_{i=1;k=1;2;3;4}(f_{12})$ characterizes the fluorescence of linear oscillators arising as a result of optically anisotropic absorption. Elements $r_{i=2;3;k=1;2;3;4}(f_{21;22;33})$ determine the phase-modulated (δ, θ) fluorescence of linear oscillators. Finally, the values of elements $r_{i=4;k=1;2;3;4}(f_{21;22;33}, f_{44})$ contain complex information about the fluorescence of linear ($f_{12;21;22;33}$) and elliptical (f_{44}) oscillators in an optically anisotropic medium with linear and circular birefringence.

It should be noted that practical usage of Eq. (8) is difficult. The reason for that consists in the azimuthal dependence of the majority of matrix elements; generally 12 out of 16 elements change while rotating the sample around the probing axis. In our case, the azimuthal dependence of the majority of Mueller-matrix elements is associated with a change in the direction of the optical axis of biological crystal $\gamma(\Theta)$. The results of research[3,5] enable us to solve this problem. It is shown that the following matrix elements are azimuthally stable, independent of the sample rotation angle (Θ):

$$\begin{cases} r_{11}(\Theta) = const; \\ r_{14}(\Theta) = const; \\ r_{41}(\Theta) = const; \\ r_{44}(\Theta) = const. \end{cases} \tag{9}$$

Analysis of Eq. (9) with regard to Eqs. (1)–(7) shows that all matrix elements $r_{11;14;41;44}$ are independent of the "orientation" parameter γ of polycrystalline networks. Along with this, the physical information concerning the fluorescence of linear ($r_{14} \leftrightarrow f_{12}$) and elliptical ($r_{41;44} \leftrightarrow f_{21;22;33}; f_{44}$) oscillators is stored in different Mueller-matrix invariants.

Thus having experimentally measured the coordinate distributions of elements ($q \equiv \{r_{14;41;44}\}$) by means of a CCD camera in the spectral range ($\lambda_f = 0.63$ to 0.65 μm), it is possible to obtain azimuthally stable information about the fluorescence of porphyrins of optically anisotropic structures of polycrystalline films of dried peritoneal fluid. This fact provides the validity of the measured data in production or screening studies.

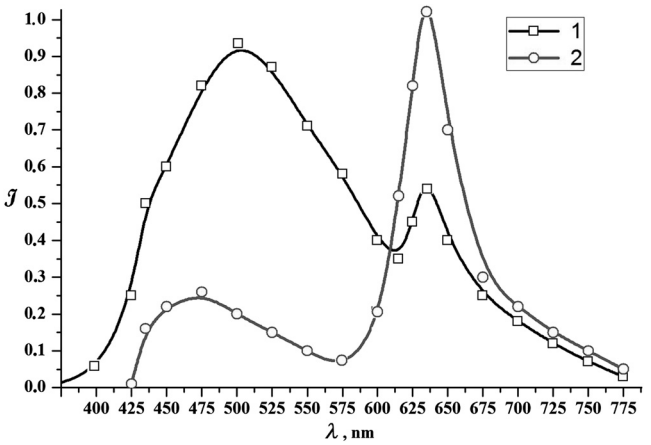

Fig. 1 Fluorescence spectra of films of dried peritoneal fluid (1) and porphyrin IX (2) under the excitation with the wavelength of $\lambda = 0.405$ μm.

3 Objects and Method of Investigation. Algorithms of Mueller-Matrix Image Processing

Optically thin (absorption coefficient $\tau < 0.1$) polycrystalline films of dried peritoneal fluid of the following two types were used as the objects of investigation:

- Healthy donors: group 1 (51 samples);
- Patients with endometriosis: group 2 (20 samples).

The samples were produced by placing a drop of peritoneal fluid onto an optically homogeneous glass followed by 24-h drying at room temperature.

At the first stage in order to determine the influence of porphyrins of a polycrystalline film of dried peritoneal fluid on the spectral dependence of the intensity of the laser-induced fluorescence, the following comparative study was performed. We measured the fluorescence spectra (excitation by the wavelength of $\lambda = 0.405$ μm) of a reference film of dried solution (porphyrin IX in ether) and the film of dried peritoneal fluid from group 1 (Fig. 1). The measurement procedure was performed by means of monochromator MDR-12 (LOMO).

Comparative analysis of obtained data shows good correlation between the spectral peaks of the fluorescence intensity of the porphyrins in both samples in the range of $\lambda_f = 0.63$ to 0.65 μm.

The measurements of coordinate distributions of Mueller-matrix elements characterizing polarization properties of polycrystalline films of peritoneal fluid were performed in the setup of the conventional Stokes polarimeter.[12] Figure 2 presents the scheme of a laser polarimeter modified for the study of autofluorescence of biological layers.

In order to induce the autofluorescence in the location of the Stokes polarimeter, we have used a "blue" semiconductor laser LSR405ML-LSR-PS-II—(1) with the wavelength $\lambda = 0.405$ μm and power $W = 50$ mW. The polarization state generator consists of quarter-wave plates (3), (5) (Achromatic True Zero-Order Waveplate) and polarizer (4) (B + W Kaesemann XS-Pro Polarizer MRC Nano). Biological layer (6) was illuminated by a laser beam with the following types of polarization: linear with azimuths 0 deg, 90 deg, +45 deg and right circulation (⊗). Images of biological layer made by strain-free objective (7) (Nikon CFI Achromat P, focal distance 50 mm, numerical aperture 0.1, and magnification 4×) were projected in the plane of light-sensitive plate of CCD-camera (11) (The Imaging Source DMK 41AU02.AS, monochrome 1/2" CCD, Sony ICX205AL [progressive scan]; resolution 1280×960; size of light-sensitive plate 5952×4464 μm; sensitivity 0.05 lx; dynamic range 8 bit, SNR 9 bit). The analysis of images of biological layers (6) was performed by means of a polarization state analyzer consisting of a polarizer (9) and quarter-wave plate (8).

Measurement of coordinate distributions of autofluorescent intensity I_λ^Φ of biological layers (6) in the plane of the light-sensitive plate of CCD camera 11 was performed using the set of bandpass interference filters (10). These filters mounted into the revolving disk provide the possibility of spectrally selective analysis of fluorescence of biological layers (6) in three regions of the spectrum: $\lambda_f^{(1)} = 0.43$ to 0.45 μm, $\lambda_f^{(2)} = 0.53$ to 0.55 μm, and $\lambda_f^{(3)} = 0.63$ to 0.65 μm.

The values of Mueller-matrix invariants, Eq. (9), were calculated by means of the following algorithm:

$$\begin{cases} r_{14} = S_1^{\otimes} - 0.5(S_1^0 + S_1^{90}); \\ r_{41} = 0.5(S_4^0 + S_4^{90}); \\ r_{44} = S_4^{\otimes} - 0.5(S_4^0 + S_4^{90}). \end{cases} \tag{10}$$

Here $S_{i=2;3;4}^{0;45;90;\otimes}$ is a Stokes vector parameter in the points of the digital image of laser polarization autofluorescence of polycrystalline films measured for a series of linearly (0 deg, 45 deg, 90 deg) and right circularly polarized (⊗) probing laser beams.

The time of one measuring cycle of the set of Mueller-matrix elements of sample does not exceed 2 min.[13]

For objective analysis of coordinate distributions of Mueller-matrix invariants $q \equiv \{r_{14;41;44}(m \times n)\}$, we used the methods of statistical analysis.[12] The set of statistical moments of the first to fourth orders which characterize distributions q was calculated using the following algorithms:

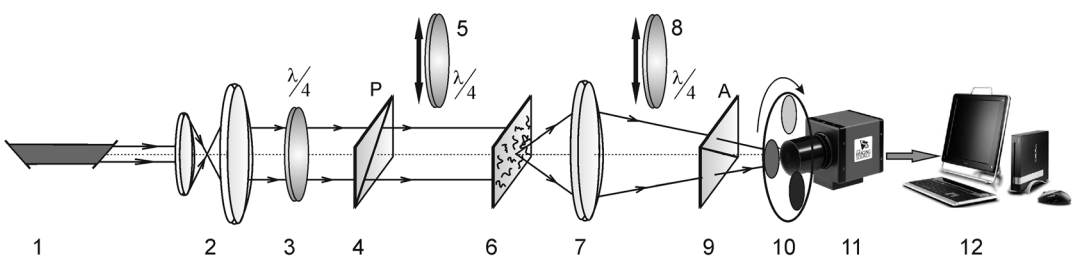

Fig. 2 Optical scheme of laser polarization autofluorescent Stokes polarimeter.

$$Z_1 = \frac{1}{N}\sum_{j=1}^{N}|q|_j; \quad Z_2 = \sqrt{\frac{1}{N}\sum_{j=1}^{N}(q - Z_1)_j^2};$$

$$Z_3 = \frac{1}{Z_2^3}\frac{1}{N}\sum_{j=1}^{N}(q - Z_1)_j^3; \quad Z_4 = \frac{1}{Z_2^4}\frac{1}{N}\sum_{j=1}^{N}(q - Z_1)_j^4, \quad (11)$$

where N is the number of pixels of the CCD camera.

4 Analysis and Discussion of Experimental Results

Figures 3 and 4 present the series of experimentally measured normalized Mueller-matrix images $r_{ik}(m \times n)/r_{11}$ characterizing laser polarization autofluorescence of optically anisotropic polycrystalline films of dried peritoneal fluid of group 1 (Fig. 3) and group 2 (Fig. 4).

The analysis of the data obtained shows the common regularity: the nonzero value of all Mueller-matrix elements characterizing polarization fluorescence of polycrystalline films of dried peritoneal fluid. Such a structure of the resulting Mueller matrix of fluorescence of polycrystalline films of dried peritoneal fluid, Eq. (8), confirms the simultaneous influence of the four mechanisms of amplitude, Eqs. (1) and (2), and phase, Eqs. (6) and (7), anisotropies on the parameters of autofluorescent radiation Eqs. (3)–(5). However, as was assumed during the model analysis, polarization autofluorescence is the most reliable in terms of reproducibility of results manifested in coordinate distributions of Mueller-matrix invariants r_{14} (fluorescence of linear oscillators), r_{41}, and r_{44} (fluorescence of linear and elliptical oscillators) of the samples of group 1 and group 2.

The series of Figures 5–7 presents the coordinate distributions of the values of autofluorescent Mueller-matrix invariants $r_{14;41;44}(m \times n)$ [(a) and (b)] and the corresponding histograms [(c) and (d)] of the samples of polycrystalline films of dried peritoneal fluid from group 1 [(a) and (c)] and group 2 [(b) and (d)].

The comparative analysis of the data obtained showed the sufficient increase of the mechanisms of autofluorescence of linear and elliptical oscillators in the case of endometriosis. This fact is confirmed by the increase in 2 to 4 times of the range of values changes [Figs. 5(d)–7(d)] of all Mueller-matrix invariants $r_{14;41;44}(m \times n)$ in comparison with (c). It can be explained physically by the increase of porphyrins concentration (linear oscillators $r_{14} \uparrow$) and formation of polycrystalline networks ($r_{41;44} \uparrow$) in dried peritoneal fluid of endometriosis patients in comparison with the group of healthy donors.

For the purpose of an objective comparative evaluation of all Mueller-matrix invariants $r_{14;41;44}(m \times n)$ in accordance with Eq. (11) at the first stage, the set of statistical moments of the first to fourth orders ($Z_{i=1;2;3;4}$) characterizing distributions $N(r_{14;41;44})$ was calculated for two patients from different

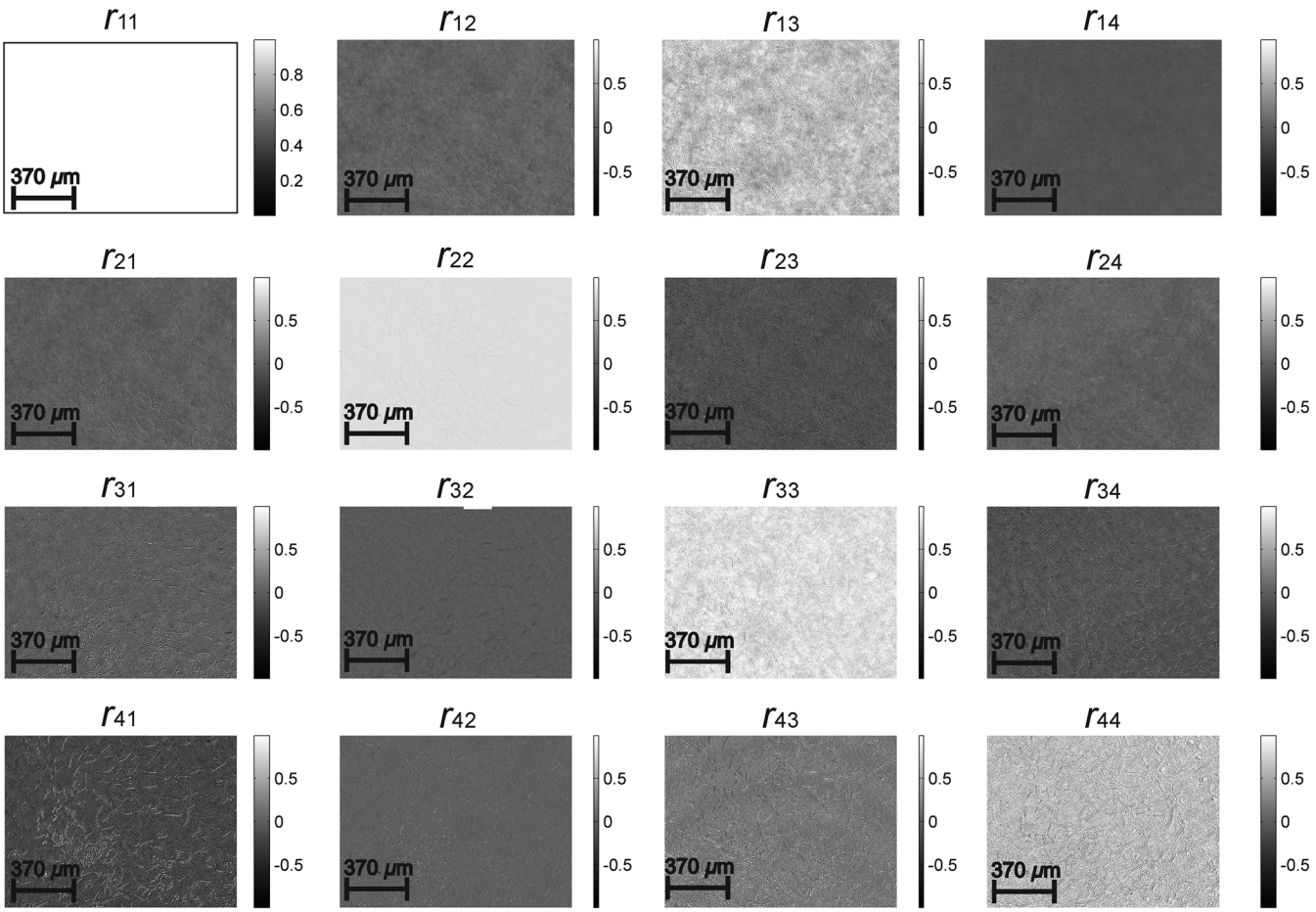

Fig. 3 Normalized autofluorescent Mueller-matrix images of polycrystalline films of dried peritoneal fluid (group 1).

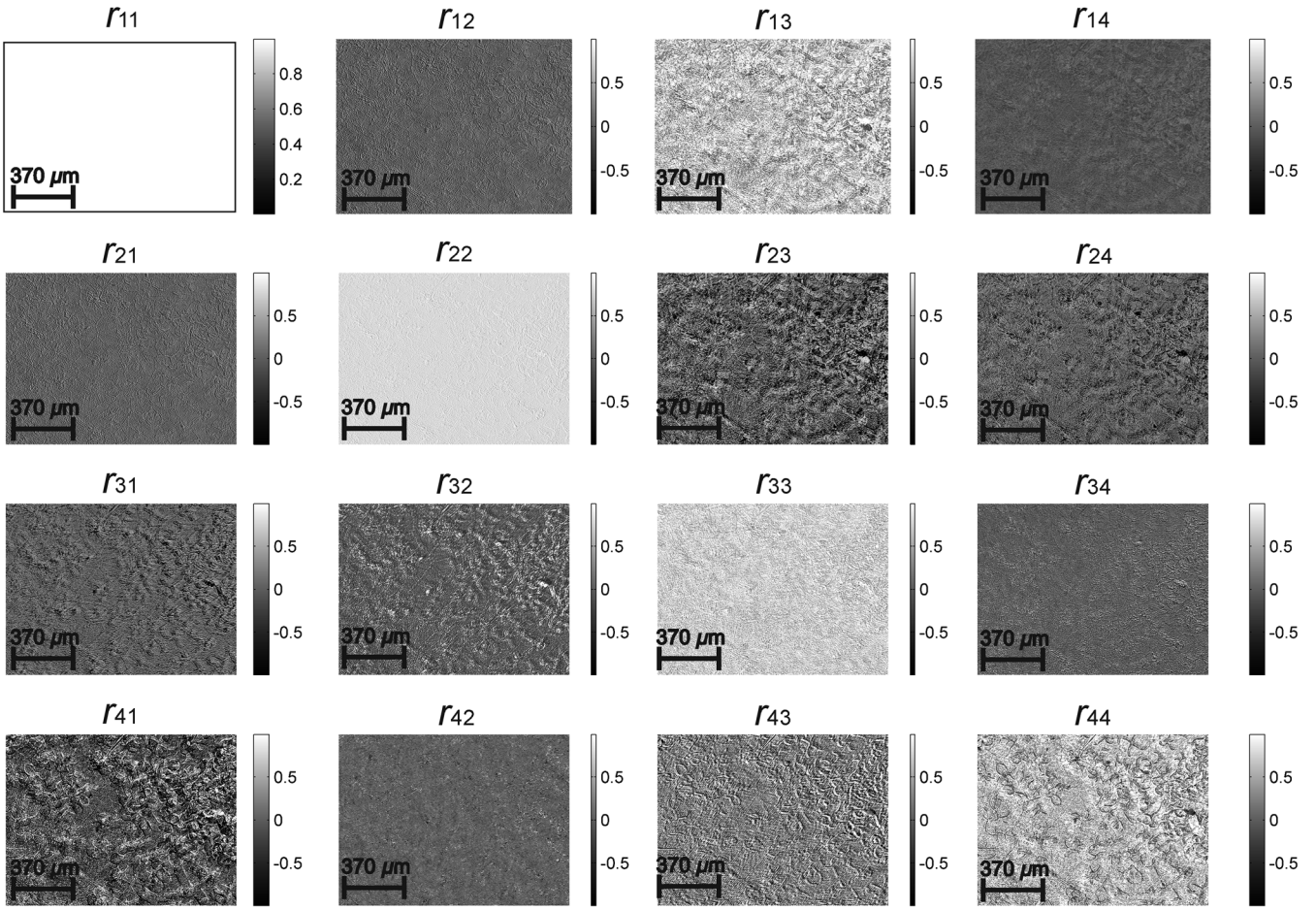

Fig. 4 Normalized autofluorescent Mueller-matrix images of polycrystalline films of dried peritoneal fluid (group 2).

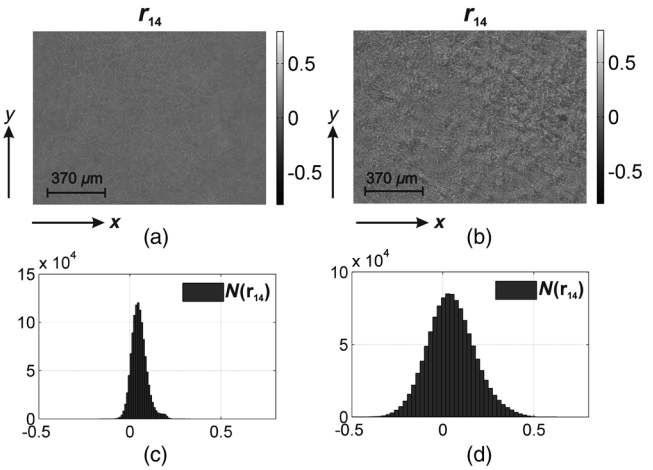

Fig. 5 (a) and (b) Autofluorescent Mueller-matrix images $r_{14}(m \times n)$ and (c) and (d) the corresponding histograms of the samples of polycrystalline films of dried peritoneal fluid from (a) and (c) group 1 and (b) and (d) group 2.

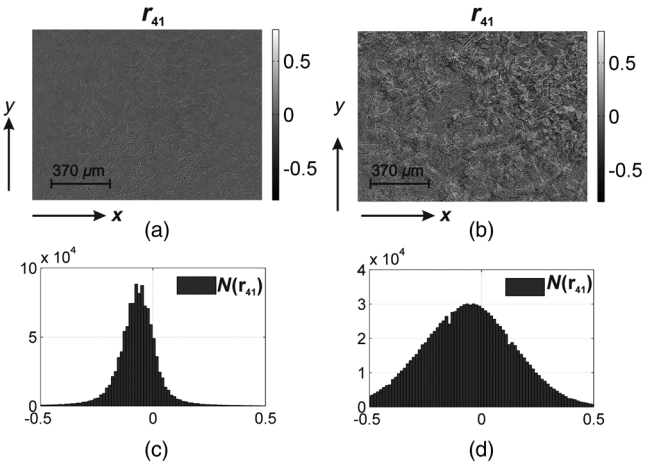

Fig. 6 (a) and (b) Autofluorescent Mueller-matrix images $r_{41}(m \times n)$ and (c) and (d) the corresponding histograms of the samples of polycrystalline films of dried peritoneal fluid from (a) and (c) group 1 and (b) and (d) group 2.

groups. Analysis of the data revealed that the statistics of all the experimentally measured two-dimensional distributions $r_{14;41;44}(m \times n)$ differ from the Gaussian or normal—all the statistical moments $Z_{i=1;2;3;4} \neq 0$ (see Table 1).

This fact is well correlated with the results of polarization and Mueller-matrix mapping of histological sections of biological tissues (skin, tissues of reproductive system of women, myocardium, and others) and polycrystalline films of dried

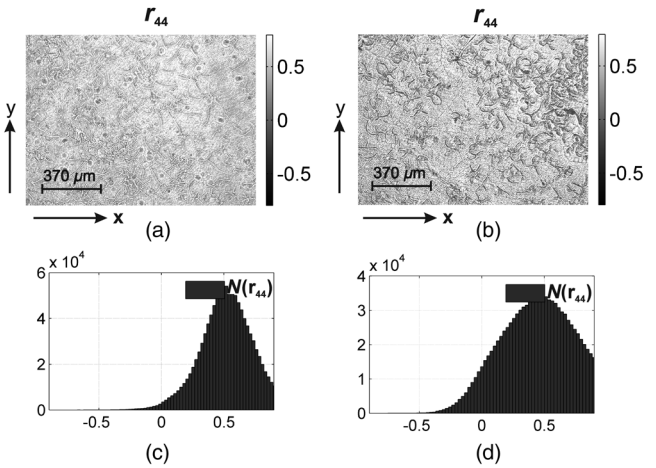

Fig. 7 (a) and (b) Autofluorescent Mueller-matrix images $r_{44}(m \times n)$ and (c) and (d) the corresponding histograms of the samples of polycrystalline films of dried peritoneal fluid from (a) and (c) group 1 and (b) and (d) group 2.

biological fluids (blood plasma, synovial fluid, bile, and so on) of oncologically changed human organs.[11,12] This shows that the most sensitive to such changes are the statistical moments of higher orders $Z_{i=3;4}$. The range of changes in their value (tumor biopsy) is 3 to 5 times greater than the range of change of the mean (Z_1) and dispersion (Z_2). In our case (peritoneal fluid of healthy patients and with endometriosis) the histograms of distributions $N(r_{14;41;44})$, although they differ from normal (group 1), are still quite symmetrical (group 2). Therefore, the values of the skewness (Z_3) and the kurtosis (Z_4) of such distributions are comparable with the values of the statistical moments of the first and the second orders.

Table 1 Statistical ($Z_{i=1;2;3;4}$) moments of the first to fourth orders of the distribution of Mueller-matrix invariants of polycrystalline films of dried peritoneal fluid of one patient from group 1 (healthy donor) and one patient from group 2 (endometriosis patient).

	r_{14}		r_{41}		r_{44}	
Z_i	Group 1	Group 2	Group 1	Group 2	Group 1	Group 2
Z_1	0.08	0.12	0.13	0.23	0.45	0.54
Z_2	0.07	0.23	0.15	0.38	0.23	0.34
Z_3	0.51	0.18	0.21	0.09	0.31	0.13
Z_4	0.71	0.21	0.29	0.08	0.25	0.11

Table 3 Operational characteristics of the method of Mueller-matrix mapping of autofluorescence of polycrystalline films of dried peritoneal fluid.

Parameter	Z_i	r_{14}	r_{41}	r_{44}
$Ac(Z_i)$	Z_1	79%	82%	72%
	Z_2	95%	91%	75%
	Z_3	96%	85%	86%
	Z_4	92%	95%	82%

For the possible clinical application of both methods, the following parameters were determined for each group of samples:[39–41]

- Mean values of statistical moments $\bar{Z}_{i=1;2;3;4}(q)$, their standard deviations $\sigma_{i=1;2;3;4}(q)$, and histograms $N(\bar{Z}_i)$ within groups 1 and 2 (see Table 2).
- Operational characteristics traditional for probative medicine[42,43] are sensitivity ($Se = \frac{a}{a+b}100\%$), specificity ($Sp = \frac{c}{c+d}100\%$), and balanced accuracy ($Ac = \frac{Se+Sp}{2}$), where a and b are the number of correct and wrong diagnoses within group 2; c and d are the same within group 1 (see Table 3).

Differences between the statistical sets $Z_{i=1;2;3;4}(q)$ were significant in the case when the average value $\bar{Z}_{i=1;2;3;4}(q)$ within group 1 did not "overlap" with the range $1.96 \times \sigma_{i=1;2;3;4}(q)$ (this provides 95% of confidence interval) within group 2 and vice versa.[39–41]

The comparative analysis of the obtained data (Table 1) showed that the differences between the values of average $\bar{Z}_{i=1;2;3;4}$ moments of all orders are statistically valid.

The comparative analysis of operational characteristics of the method of Mueller-matrix mapping of autofluorescence of polycrystalline films of dried peritoneal fluid showed the following optimal parameters (highlighted in gray) for differentiation of biological layers of all types. The obtained results enable us to assert that the level of accuracy of the suggested

Table 2 Statistical ($\bar{Z}_{i=1;2;3;4} \pm 1.96\sigma_{i=1;2;3;4}$) moments of the first to fourth order distribution of Mueller-matrix invariants of polycrystalline films of dried peritoneal fluid—group 1 (healthy donors) and group 2 (endometriosis patients).

	r_{14}		r_{41}		r_{44}	
Z_i	Group 1	Group 2	Group 1	Group 2	Group 1	Group 2
Z_1	0.09 ± 0.007	0.14 ± 0.011	0.12 ± 0.008	0.21 ± 0.014	0.49 ± 0.033	0.57 ± 0.041
Z_2	0.08 ± 0.005	0.28 ± 0.019	0.14 ± 0.011	0.41 ± 0.029	0.25 ± 0.013	0.33 ± 0.022
Z_3	0.62 ± 0.049	0.17 ± 0.012	0.23 ± 0.015	0.11 ± 0.08	0.34 ± 0.023	0.15 ± 0.011
Z_4	0.78 ± 0.054	0.22 ± 0.015	0.31 ± 0.022	0.09 ± 0.006	0.28 ± 0.017	0.12 ± 0.007

method is rather high. According to the criteria of probative medicine,[42,43] the parameters $Ac(Z_i) \sim 90\% - 95\%$ correspond to high quality.

5 Conclusions

The Mueller-matrix model of fluorescence of polycrystalline films of dried biological fluids of human organs with amplitude and phase anisotropies was suggested.

The Mueller-matrix invariants characterizing the polarization manifestations of fluorescence of the linear and elliptical oscillators in an optically anisotropic medium with phase (birefringence) and amplitude (dichroism) anisotropy were determined.

Within the statistical approach, the research on the efficiency of the Mueller-matrix mapping technique for laser-induced autofluorescence of polycrystalline films of dried peritoneal fluid in diagnostics of endometriosis was performed and the high quality of the diagnostic test was demonstrated.

References

1. M. Shribak and R. Oldenbourg, "Techniques for fast and sensitive measurements of two-dimensional birefringence distributions," *Appl. Opt.* **42**, 3009–3017 (2003).
2. D. Li et al., "Influence of absorption in linear polarization imaging of melanoma tissues," *J. Innov. Opt. Health Sci.* **7**, 1450009 (2014).
3. M. H. Smith, "Interpreting Mueller matrix images of tissues," *Proc. SPIE* **4257**, 82–89 (2001).
4. X. Wang and L. V. Wang, "Propagation of polarized light in birefringent turbid media: a Monte Carlo study," *J. Biomed. Opt.* **7**, 279–290 (2002).
5. S. Lu and R. A. Chipman, "Interpretation of Mueller matrices based on polar decomposition," *J. Opt. Soc. Am. A* **13**, 1106–1113 (1996).
6. O. Panchuk et al., "IV group dopant compensation effect in CdTe," *J. Cryst. Growth* **197**, 607–611 (1999).
7. Y. Wang et al., "Differentiating characteristic microstructural features of cancerous tissues using Mueller matrix microscope," *Micron* **79**, 8–15 (2015).
8. J. M. Bueno and M. C. W. Campbell, "Polarization properties of the in vitro old human crystalline lens," *Oph. Phys. Opt.* **23**, 109–118 (2003).
9. Y. Wang et al., "Study on the validity of 3×3 Mueller matrix decomposition," *J. Biomed. Opt.* **20**, 065003 (2015).
10. T. T. Tower and R. T. Tranquillo, "Alignment maps of tissues: II. Fast harmonic analysis for imaging," *Biophys. J.* **81**, 2964–2971 (2001).
11. O. V. Angel'skiĭ et al., "Structure of matrices for the transformation of laser radiation by biofractals," *Quantum Electron.* **29**, 1074–1077 (1999).
12. Y. A. Ushenko et al., "Diagnostics of structure and physiological state of birefringent biological tissues: statistical, correlation and topological approaches," in *Handbook of Coherent-Domain Optical Methods*, pp. 107–148, Springer Science+Business Media, New York (2013).
13. Y. A. Ushenko et al., "Diagnostics of optical anisotropy changes in biological tissues using Müller matrix," *Quantum Electron.* **41**, 273–277 (2011).
14. Y. A. Ushenko et al., "New parameter for describing and analyzing the optical-anisotropic properties of biological tissues," *J. Innov. Opt. Health Sci.* **4**(3), 463–475 (2011).
15. Y. A. Ushenko, "Investigation of formation and interrelations of polarization singular structure and Mueller-matrix images of biological tissues and diagnostics of their cancer changes," *J. Biomed. Opt.* **16**, 066006 (2011).
16. A. Pierangelo et al., "Ex-vivo characterization of human colon cancer by Mueller polarimetric imaging," *Opt. Express* **19**, 1582-1593 (2011).
17. T. Novikova et al., "The origins of polarimetric image contrast between healthy and cancerous human colon tissue," *Appl. Phys. Lett.* **102**, 241103 (2013).
18. A. Pierangelo et al., "Polarimetric imaging of uterine cervix: a case study," *Opt. Express* **21**, 14120–14130 (2013).
19. D. Arifler et al., "Light scattering from collagen fiber networks: micro-optical properties of normal and neoplastic stroma," *Biophys. J.* **92**, 3260–3274 (2007).
20. J. Soni et al., "Quantitative fluorescence and elastic scattering tissue polarimetry using an Eigenvalue calibrated spectroscopic Mueller matrix system," *Opt. Express* **21**, 15475–15489 (2013).
21. K. T. Schomacker et al., "Ultraviolet laser-induced fluorescence of colonic tissue: basic biology and diagnostic potential," *Lasers Surg. Med.* **12**, 63–78 (1992).
22. L. Bachmann et al., "Fluorescence spectroscopy of biological tissues—a review," *Appl. Spectrosc. Rev.* **41**, 575–590 (2006).
23. M. Lualdi et al., "Natural fluorescence spectroscopy of human blood plasma in the diagnosis of colorectal cancer: feasibility study and preliminary results," *Tumori* **93**, 567–571 (2007).
24. R. Kalaivani et al., "Fluorescence spectra of blood components for breast cancer diagnosis," *Photomed. Laser Surg.* **26**, 251–256 (2008).
25. V. Masilamani et al., "Cancer detection by native fluorescence of urine," *J. Biomed. Opt.* **15**, 057003 (2010).
26. K. M. Kadish, K. M. Smith, and R. Guilard, eds, *The Porphyrin Handbook*, Vol. **I-XX**, Academic Press, New York (2003).
27. H. Schneckenburger et al., "Fluorescence spectra and microscopic imaging of porphyrins in single cells and tissues," *Laser Med. Sci.* **4**, 159–166 (1989).
28. I. Seo et al., "Fluorescence spectroscopy for endogenous porphyrins in human facial skin," *Proc. SPIE* **7161**, 716103 (2009).
29. A. H. Gharekhan et al., "Characteristic spectral features of the polarized fluorescence of human breast cancer in the wavelet domainm," *Appl. Spectrosc.* **66**, 820–827 (2012).
30. J. Jagtap et al., "Quantitative Mueller matrix fluorescence spectroscopy for precancer detection," *Opt. Lett.* **39**, 243–246 (2014).
31. S. K. Mohanty et al., "Depolarization of autofluorescence from malignant and normal human breast tissues," *Appl. Opt.* **40**, 1147–1154 (2001).
32. D. O'Callaghan, "Endometriosis—an update," *Aust. Fam. Physician* **35**, 864–867 (2006).
33. P. Hillemanns et al., "Assessment of 5-aminolevulinic acid-induced porphyrin fluorescence in patients with peritoneal endometriosis," *Am. J. Obstet. Gynecol.* **183**, 52–57 (2000).
34. E. Auksorius et al., "Analysis of fluorescence excitation emission matrices of endometrial tissue," *Proc. SPIE* **5610**, 83 (2004).
35. G. S. Weissman et al., "Flow cytometry. A new technique in the diagnosis of malignant ascites," *J. Clin. Gastroenterol.* **9**, 599–602 (1987).
36. S. N. Savenkov et al., "Generalized matrix equivalence theorem for polarization theory," *Phys. Rev. E* **74**, 605–607 (2006).
37. Y. Shindo and Y. Oda, "Mueller matrix approach to fluorescence spectroscopy. Part I: Mueller matrix expressions for fluorescent samples and their application to problems of circularly polarized emission spectroscopy," *Appl. Spectrosc.* **46**, 1251–1259 (1992).
38. O. Arteaga, S. Nicols, and B. Kahr, "Mueller matrices in fluorescence scattering," *Opt. Lett.* **37**, 2835–2837 (2012).
39. L. D. Cassidy, "Basic concepts of statistical analysis for surgical research," *J. Surg. Res.* **128**, 199–206 (2005).
40. C. S. Davis, *Statistical Methods for the Analysis of Repeated Measurements*, Springer-Verlag, New York (2002).
41. A. Petrie and B. Sabin, *Medical Statistics at a Glance*, Blackwell Publishing Ltd., Osney Mead, Oxford (2005).
42. S. P. Robinson, *Principles of Forensic Medicine*, Cambridge University Press, Cambridge, New York (1996).
43. A. G. Lalkhen and A. McCluskey, "Clinical tests: sensitivity and specificity," *Contin. Educ. Anaesth Crit. Care Pain* **8**, 221–223 (2008).

Yuriy A. Ushenko received his doctorate degree in physics and mathematics, and his PhD in biomedical optics. He is an associate professor at the Correlation Optics Department, Chernivtsi National University. He is an author of over 100 scientific articles, 5 monographs, and 30 patents. His area of expertise is biomedical optics, including multifunctional polarization-correlation microscopy and laser autofluorescent polarimetry of optically anisotropic biological layers.

Galina D. Koval received her PhD in medicine. She is an associate professor at the Department of Clinical Immunology, Allergology, and Endocrinology, Bukovinian State Medical University. She is an author

of over 30 scientific articles and 2 patents. Her area of expertise is the Mueller and Stokes polarimetry of biological tissues and fluids.

Alexander G. Ushenko received his doctorate degree in physics and mathematics. He is a professor and the head of the Department of Optics and Spectroscopy at Chernivtsi National University. He is an author of over 150 scientific articles, 14 monographs, and 37 patents. His areas of expertise are polarimetry of biological tissues and fluids, and autofluorescence polarimetry.

Olexander V. Dubolazov received his PhD in biomedical optics. He is an associate professor at the Department of Optics and Spectroscopy, Chernivtsi National University. He is an author of over 50 scientific articles, 14 monographs, and 4 patents. His area of expertise is the Mueller-matrix polarimetry of biological tissues and fluids.

Vladimir A. Ushenko received his PhD in biomedical optics. He is an assistant professor at the Correlation Optics Department, Chernivtsi National University. He is an author of over 50 scientific articles and 3 patents. His area of expertise is the Mueller-matrix polarimetry of biological tissues and fluids.

Olga Yu. Novakovskaya received her PhD in biomedical optics. She is an assistant professor at the Department of Medical Physics and Biological Informatics, Bukovinian State Medical University. She is an author over of 30 scientific articles and 2 patents. Her area of expertise is the Mueller-matrix polarimetry of biological tissues and fluids.